American Mineralogist, Volume 84, pages 1071–1079, 1999

Oxidation state of gold and arsenic in gold-bearing arsenian pyrite

GRIGORE SIMON,[1,*] HUI HUANG,[2] JAMES E. PENNER-HAHN,[2] STEPHEN E. KESLER,[1,†] AND LI-SHUN KAO[1]

[1]Department of Geological Sciences, University of Michigan, 2534 C.C. Little Building, Ann Arbor, Michigan 48109, U.S.A.
[2]Department of Chemistry, University of Michigan, 930 North University Avenue, Ann Arbor, Michigan 48109, U.S.A.

ABSTRACT

XANES measurements on gold-bearing arsenian pyrite from the Twin Creeks Carlin-type gold deposits show that gold is present as both Au^0 and Au^{I+} and arsenic is present at As^{I-}. Au^0 is attributed to sub-micrometer size inclusions of free gold, whereas Au^{I+} is attributed to gold in the lattice of the arsenian pyrite. STEM observations suggest that As^{I-} is probably concentrated in angstrom-scale, randomly distributed layers with a marcasite or arsenopyrite structure. Ionic gold (Au^{I+}) could be concentrated in these layers as well, and is present in both twofold- and fourfold-coordinated forms, with fourfold-coordinated Au^{I+} more abundant. Twofold-coordinated Au^{I+} is similar to gold in Au_2S in which it is linearly coordinated to two sulfur atoms. The nature of fourfold-coordinated Au^{I+} is not well understood, although it might be present as an Au-As-S compound where gold is bonded in fourfold coordination to sulfur and arsenic atoms, or in vacancy positions on a cation site in the arsenian pyrite. Au^{I+} was probably incorporated into arsenian pyrite by adsorption onto pyrite surfaces during crystal growth. The most likely compound in the case of twofold-coordinated Au^{I+} was probably a tri-atomic surface complex such as S_{pyrite}-Au^{I+}-$S_{bi\text{-}sulfide}H$ or Au^{I+}-S-Au^{I+}. The correlation between gold and arsenic might be related to the role of arsenic in enhancing the adsorption of gold complexes of this type on pyrite surfaces, possibly through semiconductor effects.

INTRODUCTION

Carlin-type gold deposits are of interest to the mineralogical community because of the unusual and still poorly understood setting for the gold they contain. Knowledge of the form of gold in these deposits is important to understanding the relevant chemical reactions, the origin of these deposits and the geological models that guide exploration for them. It is also important in developing cost-effective methods to recover gold from the ores.

Carlin-type deposits contain pyrite, other sulfide or gangue minerals, and organic matter, all of which are potential hosts for gold (Hausen and Kerr 1968; Radtke et al. 1972; Hausen 1981). Organic matter has low gold contents and plays a passive role in gold deposition (e.g., Hausen and Park 1985; Radtke 1985; Kettler 1990). SEM/electron microprobe, synchrotron radiation-induced X-ray fluorescence, and Auger/high resolution transmitted electron microscopy (HRTEM) analyses show that illite and quartz are not important hosts for gold (Chao et al. 1986; Hausen et al. 1987; Bakken et al. 1989). Wells and Mullens (1973) and Radtke (1985) had found detectable levels of gold and arsenic in small grains of pyrite or thin overgrowths of pyrite on earlier large pyrite grains. Subsequent ion probe (SIMS) analyses (Chryssoulis 1990; Bakken et al. 1991b; Arehart et al. 1993; Sha 1993) showed that arsenic-rich pyrite (arsenian pyrite) is the dominant host for gold in Carlin-type deposits. Cline et al. (1997) and Simon et al. (1997, 1999) confirmed the importance of arsenian pyrite as a host for gold in Carlin-type deposits, and Simon et al. (1999) reported that it contained as much as 1465 ppm gold.

Pyrite could incorporate Au through various mechanisms including solid solution or minute inclusions of gold or gold-bearing minerals. Bakken et al. (1989) used Auger and HRTEM to detect 50 to 200 Å gold inclusions in arsenian pyrite, whereas Bakken et al. (1991b), Arehart et al. (1993), and Sha (1993) interpreted SIMS and TEM observations to indicate that gold was homogeneously distributed in arsenian pyrite. Bakken et al. (1991b) and Arehart et al. (1993) noted that the ion beam could not resolve gold-bearing inclusions smaller than about 20 Å, but that significant heterogeneity in Au distribution would likely be observed in SIMS traverses if most gold was present entirely in inclusions rather than in a more dispersed form such as solid solution. Ion probe analyses of arsenian pyrite showed a positive correlation between Au and As concentrations (Cook and Chryssoulis 1990; Bakken et al. 1991a, 1991b; Arehart et al. 1993; Fleet et al. 1993; Fleet and Mumin 1997) and an apparently negative correlation between Au and Fe (Fleet and Mumin 1997). On the basis of these observations and preliminary X-ray photoelectron spectroscopic measurements, Arehart et al. (1993) suggested Au^{3+} entered the arsenian pyrite structure through coupled substitution for Fe and As, whereas Sha (1993) suggested that Au(HS) was adsorbed onto the surface of arsenian pyrite.

*Present address: Shell International Exploration and Production B.V., Carel van Bylandtlaan 16, The Hague, The Netherlands.
†E-mail: skesler@umich.edu

Evaluation of these possibilities requires information on the oxidation state of gold in the pyrite. Spectroscopic studies have yielded ambiguous results on the oxidation state of gold in arsenopyrite and arsenian pyrite from other types of deposits. Mössbauer studies indicate that Au is present in arsenopyrite and arsenian pyrite in a "combined" (structurally bound) state (Marion et al. 1986, 1991a, 1991b; Wagner et al. 1986, 1988, 1989; Cathelineau et al. 1989; Friedl et al. 1991; Friedl 1993), but no precise information was obtained on the oxidation state of gold, its neighbor atoms, or the type of bonding in the structure of these minerals. Using Mössbauer spectroscopy and the analogy with PtX_2 chalcogenides and pnictides (X = S, Se, Te, As, Sb), Friedl et al. (1995) suggested that chemically bound gold in arsenopyrite and pyrite occupies iron sites in their lattices. In this configuration, gold with an unknown oxidation state would be coordinated by six sulfur atoms in pyrite and by three sulfur and three arsenic atoms in arsenopyrite. Tossell et al. (1981) suggested that sulfur and arsenic form pairs of atoms, occurring as S_2^{2-} in pyrite and AsS^{2-} in arsenopyrite.

This paper uses X-ray absorption near-edge structure (XANES), extended X-ray absorption fine structure (EXAFS), and TEM measurements made to determine the oxidation state and the position of gold and arsenic in gold-bearing pyrite from Twin Creeks, Nevada.

Samples from the Twin Creeks deposit

This typical, large Carlin-type deposit in northwestern Nevada, produces about 500 000 ounces of gold annually. Pyrite used here was obtained from the northernmost part of the Twin Creeks deposit (north of the TC fault in the northern half of the Megapit at Rabbit Creek) (Fig. 1). Mineralization and paragenesis are discussed by Simon et al. (1997, 1999) and Stenger et al. (1998). Briefly, deposition of pyrite is thought to have caused deposition of gold by destabilization of the $Au(HS)_2^-$ complex that is presumed to have carried the gold in solution. Cross-cutting relations suggest that the Twin Creeks deposit was the site of a series of six hydrothermal events or stages. Pyrite in stages 2 through 5 is found as overgrowths on earlier pyrite or very fine-grained aggregates of small crystals with a porous texture (Simon et al. 1997, 1999). SIMS analyses of these pyrites indicated that gold concentrations are highest in pyrite with the smallest grain sizes (Simon et al. 1999) we examined here.

CTW-150/898 and CTW-158/807 contain pyrite from the Stage 2 assemblage associated with adularia. CTW-5/864 and

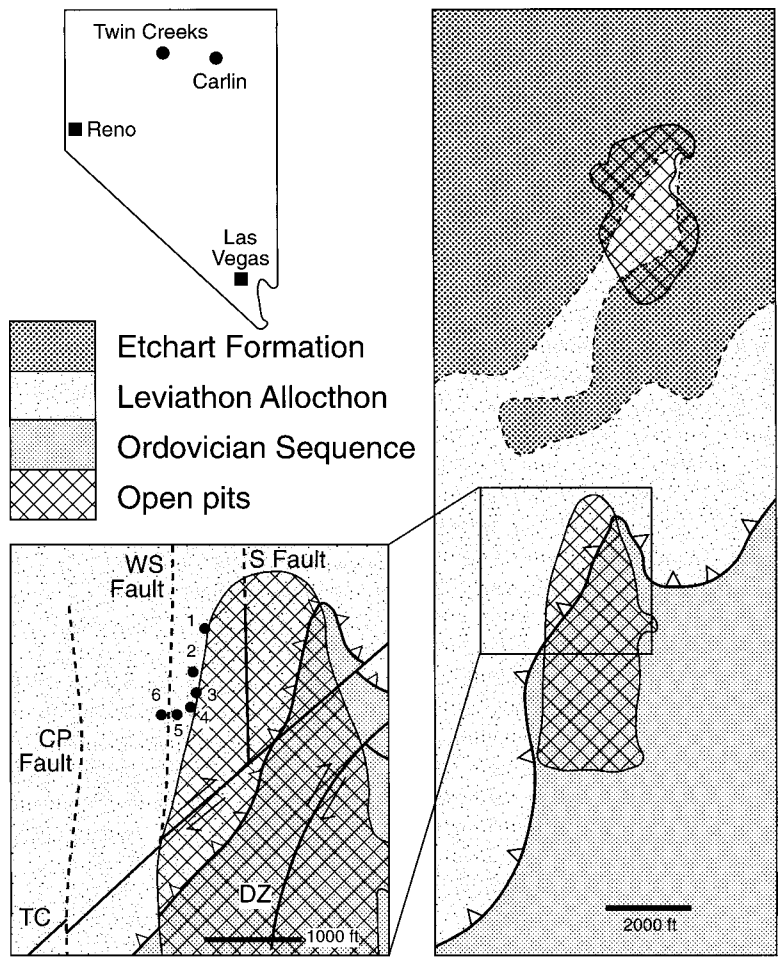

FIGURE 1. Location of the Twin Creeks deposit in Nevada, showing the relation between the Rabbit Creek or Megapit deposit (southern open pit) where samples described here were obtained and other mineralization at Chimney Creek or Vista-Discovery Pits (northern open pit). Map modified from Stenger et al. (1998). Lower left inset shows location of samples in the northern part of the Megapit. Note: CP Fault = Central Pacific fault, DZ = DZ fault, S Fault = Sage fault, TC = Twin Creeks fault, WS Fault = West Side fault, List of samples (drill hole number and depth in feet): 1 = CTW 197/805, 2 = CTW 158/807, 3 = CTW 150/898, 4 = CTW 5/864, 5 = CTW 32/776, 6 = CTW 12/822.

CTW-32/776 contain pyrite from the Stage 2 assemblage associated with illite with or without quartz. Samples CTW-12/822.2 and CTW-197/805 contain arsenian pyrite from Stage 5 mineralization, which was the last gold-bearing stage to be deposited at Twin Creeks. Figure 2 shows micrographs of the samples.

These samples have relatively high gold grades and an absence of other sulfides (determined from microscopic examination). Hand specimens were collected from 5 foot sections of drill core with very high assay values for gold; individual hand samples were not analyzed for gold. Arsenian pyrite was concentrated from crushed material by hand picking with tweezers under a binocular microscope. Material from the pre-concentration stage was crushed to pass 100 mesh and washed in distilled water. This process yielded arsenian pyrite concentrates that contained as much as 30% silicate material. The only sulfide contaminant in most samples was pre-ore pyrite, which could not be separated from arsenian pyrite, although it is considerably less abundant than ore-related pyrite in the samples used for our analyses, and made up the interior rather than the surface of most grains.

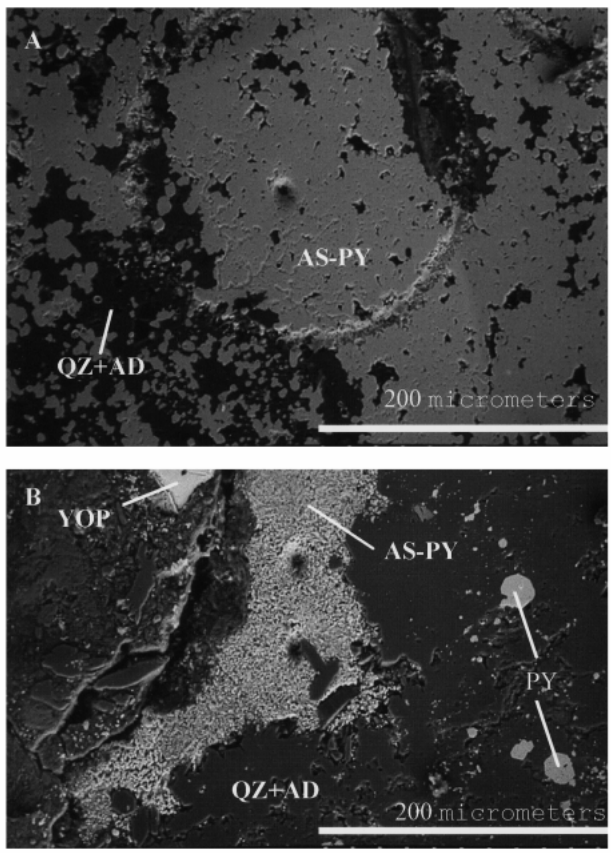

FIGURE 2. BSE images of **(a)** arsenian pyrite (AS-PY) from Stage 2 in association with quartz and adularia (QZ+AD), and **(b)** arsenian pyrite (AS-PY) from Stage 5 cutting the quartz-adularia assemblage (QZ+AD) from Stage 2. Yellow orpiment (YOP) represents Stage 6 of mineralization and pyrite (PY) is pre-ore pyrite.

ANALYTICAL METHODS

For XANES and EXAFS analyses, arsenian pyrite concentrates were mounted onto glass slides to cover an area of 15×1 mm, the cross section of the X-ray beam. Spectra were measured at the Au L_{III}-edge at 10 Kelvin. Gold spectra were measured in fluorescence mode using a 13-element solid state detector at the Stanford Synchrotron Radiation Laboratory (SSRL) beamline VII-3 (3.0 GeV, 100 mA). A Si (220) double-crystal monochromator was used and was detuned 50% for harmonic rejection. Spectra were calibrated using a gold foil internal standard, with the first inflection point of the foil edge defined as 11919 eV. Data were analyzed using standard procedures for normalization, with the modification that the underlying arsenic K-edge spectrum at ca. 11867 eV was subtracted from the gold data using fluorescence mode measurements of the As K-edge as a reference spectrum.

Standards were gold foil for Au^0, Au^{I+}_2S, and $Na_3Au^{I+}(S_2O_3)_2$ for Au^{I+} with CN of 2 $[Au^{I+}(PPh_2Me)_4]PF_6$, and $[Au^{I+}(CH_3CN)_4]ClO_4$ for tetrahedrally coordinated Au^{I+},, and $NaAu^{III}Cl_4$ for Au^{3+} in square planar coordination. XANES spectra for Au^{I+}_2S, $Na_3Au^{I+}(S_2O_3)_2$, and $NaAu^{III}Cl_4$ were obtained here, whereas the XANES spectra of $[Au^{I+}(PPh_2Me)_4]PF_6$ and $[Au^{I+}(CH_3CN)_4]ClO_4$ were taken from Elder and Eidsness (1987) and Ahrland et al. (1989), respectively. Au^{I+}_2S and $Na_3Au^{I+}(S_2O_3)_2$ standards were purchased from Aldrich Chemicals and Alfa Aesar, respectively. Because Au^{I+}_2S is a metastable compound, its XANES and EXAFS spectra were obtained immediately after the sample was made to avoid problems associated with decomposition of the compound. XANES and EXAFS spectra of gold in the Au^{I+}_2S standard taken at the same time with those of gold in arsenian pyrite, show that the degree of decomposition of Au^{I+}_2S to Au^0 was minor (e.g., less than 5%) (Fig. 3) at the time when XANES analyses were made.

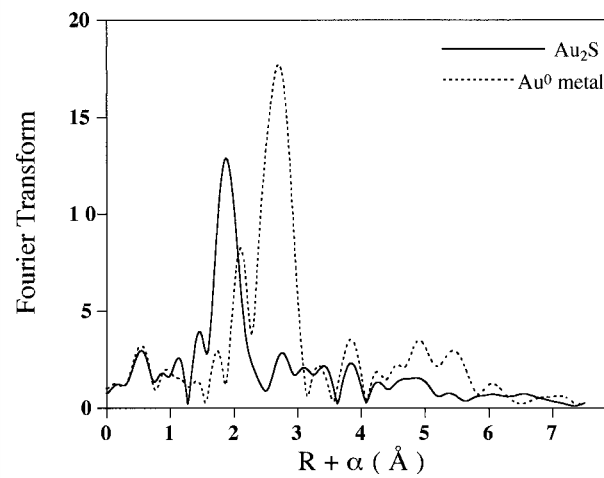

FIGURE 3. Fourier transforms (FTs) of the extended X-ray absorption fine structure (EXAFS) spectra for Au^{I+}_2S and metallic gold foil (Au^0). Transforms were calculated using k^3 weighted data for k = 1.0–13.8 Å^{-1}. The absence of a significant intensity peak at R+α ~ 2.7 Å in Au_2S demonstrates that there is insignificant decomposition to Au^0 in the analyzed Au_2S sample. (R+α, signifies that the FTs are pseudo-radial distribution functions with a phase shift α of ca. 0.4–0.5 Å).

An XRD pattern of the Au^{I+}_2S standard obtained four months after the XANES and EXAFS analyses were made is consistent with a cubic structure (space group *Pn*3*m*) reported by Hirsch et al. (1966) and Cardile et al. (1993), with a cell parameter *a* of 5.023 Å (Fig. 4). The XRD pattern also shows a small Au^0 peak, suggesting that decomposition of the sample had begun. Table 1 lists first-peak energy positions.

In reading this report, it should be kept in mind that details of the relationship between formal oxidation state and true charge are extremely complex. They are, in fact, probably not even uniquely defined, because the "charge" that is calculated for an atom depends critically on criteria that are used to apportion electrons between the element and its ligands, an especially ill-defined problem for covalent molecules. We have used, instead, an empirical meaning for formal oxidation state. Gold is traditionally assigned a formal oxidation state of 3+ in anionic complexes in which it is bonded to four electronegative ligands. These structures are often structurally similar, generally square-planar with relatively short bond lengths. Analogous structural similarities are found for Au^{I+} complexes. The similarities of the structures within a formal oxidation state and the structural differences between gold complexes in different formal oxidation states mean that physical measurements that are sensitive to structures, such as XANES, XPS, and Mössbauer, give similar spectra for compounds having the same formal oxidation state. This is true regardless of the charge that may be calculated by one or another computational approach.

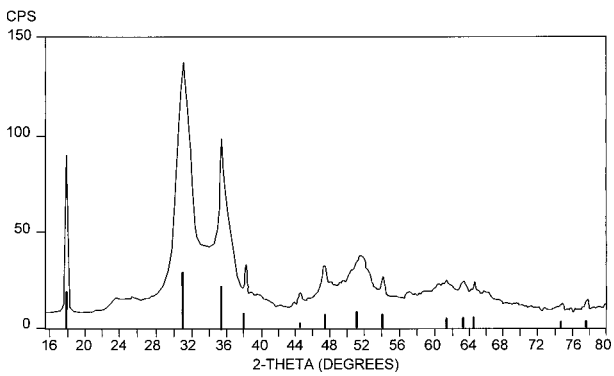

FIGURE 4. X-ray powder diffraction pattern of Au^{I+}_2S compound (using Cu*K*α radiation); labeled peaks are produced by elemental gold.

TABLE 1. First peak energies

Compound	First peak energy (eV)
Au metal	11923*
$[Au^{I+}(CH_3CN)_4]ClO_4$	11924.2
$[Au^{I+}(PPh_3Me)_4]PF_6$	11924.2
$Na_3[Au^{I+}(S_2O_3)_2]$	11923*
$NaAu^{III}Cl_4$	11918.8
CTW5/864	11922.1
CTW12/822	11923*

Notes: For standard and unknown samples used in this study listed to the nearest 0.1 eV. Sources of data not measured in this study are given in text.
* Peaks are broader and less well defined.

XANES AND EXAFS SPECTRA FOR GOLD IN ARSENIAN PYRITE

XANES spectra for gold in the arsenian pyrite samples can be divided into two groups. Arsenian pyrite samples from Stage 2 (both adularia and illite assemblages) show a high rising edge feature with a peak at 11922 eV (Fig. 5). Arsenian pyrite samples from Stage 5 have edges that are shifted about 1.0 eV to higher energy relative to the edges for arsenian pyrite samples from Stage 2 (Fig. 6). A comparison of these spectra with spectra for standards (models), including gold metal (Au^0), Au^{I+}_2S, $Na_3[Au^{I+}(S_2O_3)_2]$, $[Au^{I+}(PPh_2Me)_4]PF_6$, and $NaAu^{III}Cl_4$ (Fig. 7) suggests that the peak near 11922 eV seen in arsenian pyrite from Stage 2 represents Au^{I+} (Fig. 5). In contrast, spectra for arsenian pyrite from Stage 5 (Fig. 6) show two small peaks at 11946.1 and 11969.5 eV, which are characteristic of metallic gold with a particle size larger than ~10Å (Elder and Eidsness 1987). The presence of Au^0 in the arsenian pyrite from Stage 5 has also been confirmed by SIMS observations of sub-micrometer size inclusions of native gold (Simon et al. 1999). None of the samples appears to contain a significant amount of Au^{III}. The Au^{III} XANES spectrum has much lower energy due to the 2p→5d transition (both Au^0 and Au^{I+} have filled 5d orbitals) (Elder and Eidsness 1987).

Comparison of spectra for the different Au^{I+} samples suggests that coordination numbers of 2 (linear) and 4 (tetrahedral) can be distinguished (Fig. 7). Regardless of coordination number, all Au^{I+} spectra have a peak at approximately 11920 eV. This peak is significantly more intense for tetrahedrally coordinated Au^{I+} than it is for linearly coordinated Au^{I+}, such that the peak is lower than the edge jump for linearly coordinated, but significantly higher than the edge jump for tetrahedrally coordinated gold. In part, this observation may reflect differences in ligation for the different models (N and P for the tetrahedrally coordinated models, S for the linearly coordinated model). However, the scattering properties of P and S should be similar. A more likely explanation is that the 11920 eV peak,

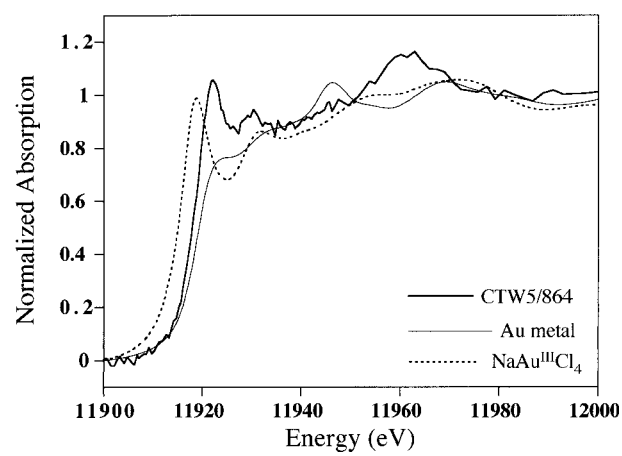

FIGURE 5. XANES spectrum for gold in arsenian pyrite sample CTW 5/685 from Stage 2. Spectrum for model compounds Au^0 and $NaAu^{III}Cl_4$ are included for comparison. Exact peak energies, which are difficult to determine directly from these plots, are listed in Table 2.

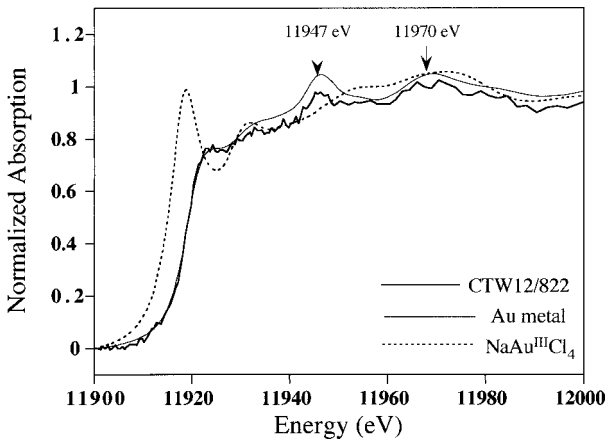

FIGURE 6. XANES spectrum for gold in arsenian pyrite sample CTW 12/822 from Stage 5, also showing spectrum for model compounds Au^0 and $NaAu^{III}Cl_4$ for comparison.

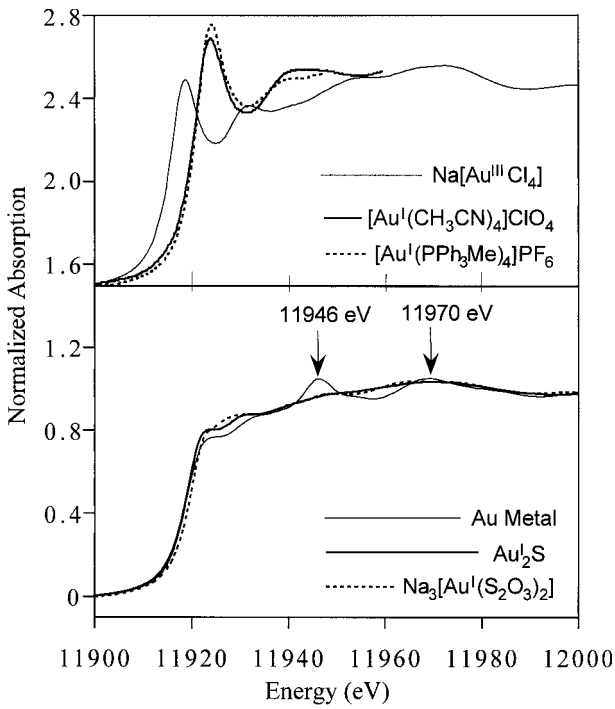

FIGURE 7. XANES spectra for gold in model compounds discussed in the text.

which arises from a "continuum resonance" transition, increases in intensity as the number of scattering atoms increases. The peak intensity at 11920 can thus be used as an approximate measure of the average coordination number of Au^{1+}. Comparison of the model spectra to those for the Twin Creeks arsenian pyrite suggests that gold in the arsenian pyrite from Stage 2 may be a mixture of linearly and tetrahedrally coordinated gold. In contrast, gold in the arsenian pyrite samples from Stage 5 yields spectra consistent with a mixture of Au^0, linearly, and tetrahedrally coordinated Au^{1+}.

The form of gold in each arsenian pyrite sample was estimated by fitting its XANES spectrum with a linear combination of three reference spectra, one for Au^0, one for linearly coordinated Au^{1+} and one for tetrahedrally coordinated Au^{1+}. The gold foil spectrum was used for Au^0. Two spectra each were used as models for linearly coordinated Au^{1+} (Au^{I}_2S and $Na_3[Au^{I+}(S_2O_3)_2]$) and tetrahedrally coordinated Au^{1+} ($[Au^{I+}(PPh_3Me)_4]PF_6$ and $[Au^{I+}(CH_3CN)_4]ClO_4$), giving a total of four ternary combinations of spectra. A total of four linear fit parameters were used: a multiplicative factor for each reference spectrum and a constant y-offset to correct for minor variations in the background subtraction. The optimized multiplicative factors were scaled to give a total Au of 100%.

Representative fits for CTW12/822 are shown in Table 2. Due to the differences in the reference spectra, the fitting results vary somewhat depending on the choice of spectra used in the fit. The apparent percentage of Au^0 and of twofold-coordinated Au^I in the sample are strongly correlated due to the relative similarity of these spectra, while the apparent percentage of fourfold-coordinated Au^I in the sample is much less sensitive to the choice of reference spectra. The overall fit quality is not particularly sensitive to the choice of model compounds (Table 2, column F). The range of percent composition values for different choices of model spectra (±10%) is taken as an estimate of the uncertainty in these fits.

The average of the percent compositions that were found for each of the sets of reference spectra are given in Table 3. Although the results are subject to a large uncertainty, they confirm that arsenian pyrite samples from Stage 2 contain negligible Au^0, while arsenian pyrite samples from Stage 5 contain significant amounts of Au^0. They suggest further that significant amounts of non-metallic gold (Au^{1+}) are present in both sample groups, with tetrahedrally coordinated Au^{1+} being more abundant than linearly coordinated Au^{1+}. The linearly coordinated Au^{1+} is similar to that in the Au^{I}_2S and $Na_3Au^{I+}(S_2O_3)_2$ standards where it is linearly coordinated by two sulfur atoms. The Au^{I}_2S structure has a single gold site in which

TABLE 2. Edge-fitting results for sample CTW-12/822

Au^{1+} models used	Au^0	Au^{1+}		Offset	Scale factor	*F*
		CN = 2	CN = 4			
$Au_2S/Au(CH_3CN)^+_4$	0.56	0.37	0.07	0.01	1.01	0.013
$Au_2S/Au(PPh_3)^+_4$	0.61	0.31	0.08	0.01	1.00	0.012
$Au(S_2O_3)^{3-}_2$/ $Au(CH_3CN)^+_4$	0.67	0.21	0.12	0.01	0.99	0.014
$Au(S_2O_3)^{3-}_2$/ $Au(PPh_3)^+_4$	0.71	0.17	0.12	0.02	1.00	0.013

Notes: Values given for Au^0 and Au^{1+} are relative abundances by which each normalized edge was multiplied to obtain the best fit to the data. Offset is the normalized background offset in absorption coefficient and scale factor is the sum of the relative abundances; both are dimensionless.

TABLE 3. Edge fitting results for gold in arsenian pyrite using raw spectra

Sample	Percentage distribution of Au oxidation state		
	Au^0	Au^{1+} (CN = 2)	Au^{1+} (CN = 4)
CTW 5/864	3	33	64
CTW 150-898	5	37	58
CTW 158/807	0	32	68
CTW 32/776	0	54	46
CTW 12/822	62	28	10
CTW 197/805	61	3	36

Notes: see text for details.

Au^{I+} is linearly bonded to two sulfur atoms (Cardile et al. 1993). $Na_2Au^{I+}As$, another compound containing linearly coordinated Au^{I+}, consists of "zigzag" chains in which the gold atoms are linearly bonded to two arsenic atoms (Mues and Schuster 1980). No XANES spectra for this compound are available to be compared with those obtained for arsenian pyrite at Twin Creeks.

XANES SPECTRA FOR ARSENIC IN ARSENIAN PYRITE

XANES spectra for arsenic in all of the Twin Creeks arsenian pyrite samples are very similar and contain two major peaks at 11 868–11 869 and 11 874 eV. They can be compared to standard spectra for natural FeAsS (arsenopyrite) and As_2S_3 (orpiment) in Figure 8. The 11868-9 eV peak observed in the Twin Creeks arsenian pyrites is similar to that observed for arsenopyrite, and suggests that arsenic in the arsenian pyrites is in a crystal setting similar to that in arsenopyrite. The 11874 eV peak observed in the arsenian pyrite XANES spectra could correspond to arsenic in a higher oxidation state, or to a multiple scattering resonance associated with lower valence arsenic. However, comparison to the standard spectra shows that neither As_2S_3 (orpiment) nor Na_3AsO_3 can account for this peak. Thus, it is likely that some arsenic is present in a more oxidized form than As^{III}, probably As^{V} in the form of arsenate (AsO_4^{3-}) units. Preliminary results that we have obtained on arsenian pyrite from other Carlin-type deposits indicate that this arsenic is present as oxidized coatings on the surface of the arsenian pyrite grains rather than as a part of the original pyrite (and thus formed under more oxidizing conditions consistent with this higher oxidation state). In arsenopyrite, the dominant oxidation state of arsenic is As^{1-} (Nesbitt et al. 1995) and it is part of the AsS^{2-} unit. It is concluded that the oxidation state of most of the arsenic in the arsenian pyrite is probably As^{1-} in a structural position similar to that in arsenopyrite, where it substitutes for sulfur in the S_2^{2-} units yielding AsS^{2-}.

CHEMICAL AND STRUCTURAL POSITION OF ARSENIC IN ARSENIAN PYRITE

Fleet et al. (1989, 1993) reported up to 8 wt% As in natural arsenian pyrite and showed that arsenic in arsenian pyrite is negatively correlated with sulfur, indicating that it is not present as native arsenic inclusions and occupies a position in the crystal lattice of the mineral. The large amount of arsenic observed in many natural arsenian pyrites contrasts with the results of dry experiments of Clark (1960) who reported no more than 0.5 wt% As in pyrite. Fleet and Mumin (1997) reported arsenic contents of up to 9.3 wt% (or 5.0 at%) in pyrite that was synthesized hydrothermally at 300 to 500 °C, but no additional information was given on the structural position of arsenic in this pyrite. It is not clear whether arsenic has a homogeneous or heterogeneous distribution in arsenian pyrite. Fleet et al. (1989) reported from X-ray evidence that no more than 0.5 mol% arsenopyrite was present in arsenian pyrite, which is considerably less than the amount of arsenopyrite needed to account for all of the arsenic in arsenian pyrite.

XRD analyses of arsenian pyrite samples from Twin Creeks did not identify any arsenopyrite, and SIMS analyses reported by Simon et al. (1999) showed that arsenic had a homogeneous distribution rather than the heterogeneous distribution that would be expected for arsenic-rich inclusions. TEM study of the same arsenian pyrite, however, shows numerous {100} planar faults, 10 to 15 Å wide, that either extend through grains or stop within them (Fig. 9). Similar planar faults in natural pyrite were interpreted as growth stacking faults (e.g., Couderec et al. 1980). Fleet et al. (1989) interpreted stacking faults observed in arsenian pyrite from Agnico-Eagle and Fairview mines as thin lamellae (only a few atoms thick) of material with a marcasite-like structure, such that (101) and (010) in marcasite are parallel to (100) and (001), respectively, in pyrite (Fayard et al. 1980). Marcasite and arsenopyrite have a marcasite-like structure and are potential candidates for the marcasite-like layers in pyrite.

The possible presence of lamellae of marcasite and/or arsenopyrite in arsenian pyrite is important because both minerals can contain much higher amounts of arsenic than pyrite. Maximum amounts of arsenic in experimentally synthesized marcasite are up to 16.5 wt% As (or 9.7 at% As), twice as much as in pyrite, whereas the amount of arsenic in arsenopyrite is up to 53.5 wt% As (or 41.5 at% As) (Fleet and Mumin 1997). The XANES spectra presented in this study show that arsenic in arsenian pyrite occupies the same sites as in arsenopyrite, where

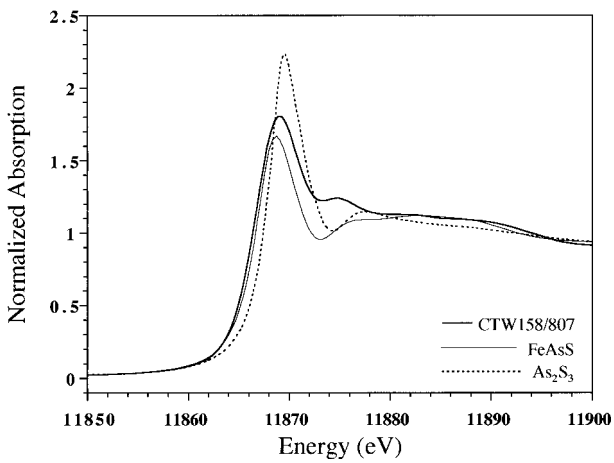

FIGURE 8. XANES spectra for arsenic in arsenian pyrite sample CTW 158/807 and standard samples FeAsS and As_2S_3.

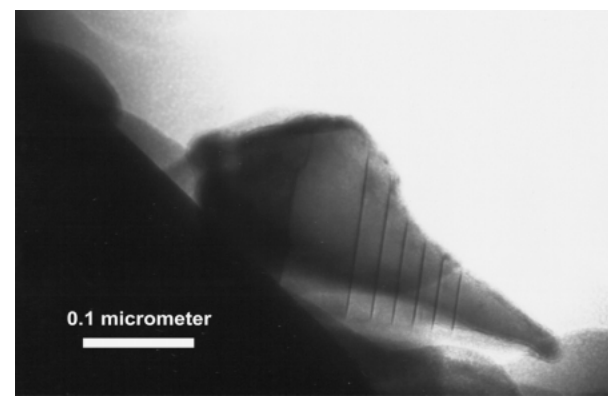

FIGURE 9. TEM image of arsenian pyrite showing stacking faults that appear as thin lamellae (10 to 12 Å wide) in pyrite.

it substitutes for sulfur (Fig. 8). Therefore, arsenic in the arsenian pyrite might be in marcasite-like layers in pyrite. Unfortunately, these "marcasite-like" layers are too small to be analyzed separately by presently available TEM or other methods. Due to their small size of 10 to 15 Å, which is equivalent to only two or three layers of marcasite or arsenopyrite, these marcasite-like lamellae are also unlikely to be detected by powder XRD analyses unless they alternate with pyrite layers in some regular way, which has not been observed in preliminary TEM studies. The irregular distribution of these marcasite-like layers in the pyrite matrix was also confirmed by HRTEM analyses of arsenian pyrite from Agnico-Eagle and Fairview mines (Fleet et al. 1989).

CHEMICAL AND STRUCTURAL POSITION OF GOLD IN ARSENIAN PYRITE

XANES analyses show that gold in arsenian pyrite from Twin Creeks is present both as Au^0 and Au^{I+}. Au^0 in arsenian pyrite is probably present as sub-micrometer size particles that do not occupy a structural position in arsenian pyrite. Gold grains of this type were reported from Carlin by Bakken et al. (1989), from Gold Quarry by Sha (1993), and from Twin Creeks by Simon et al. (1999).

Where gold in arsenian pyrite is present as Au^{I+} it apparently has two coordination numbers, two and four. The XANES spectra of arsenian pyrite that has significant Au^{I+} in twofold coordination is similar to $Au^{I+}{}_2S$, suggesting that Au^{I+} is linearly bonded to two sulfide ligands. The fourfold-coordinated Au^{I+} could be present in arsenian pyrite in one or more forms, including (1) Au^{I+} in a vacancy position on a cation site in the arsenian pyrite lattice, (2) an unknown Au-As-S compound, in which Au^{I+} is bonded in fourfold coordination to sulfur and arsenic atoms, and (3) Au^{I+} in an iron site in the pyrite structure that was deformed by substitution of one sulfur by arsenic in the S_2^{2-}. In the first setting, gold would be accompanied by point defects, and therefore its coordination would not necessarily be octahedral, as is Fe in pyrite (Fleet and Mumin 1997). In the last setting, gold might be octahedrally coordinated, but it could have four strong bonds and two weak bonds to the nearest sulfur and arsenic atoms, respectively. Presently available information does not allow discrimination among these three alternatives.

The strong correlation between gold and arsenic that has been observed in this and previous studies of arsenian pyrites (Bakken et al. 1991b; Arehart et al. 1993; Simon et al. 1999) suggests that gold is associated with the arsenic-bearing fraction of these pyrites. The arsenic-gold association has been investigated by Fleet et al. (1993) and Sha (1993), who suggested that gold is incorporated into arsenian pyrite by chemisorption onto arsenic-rich growth surfaces, and by Fleet and Mumin (1997), who used correlations among gold, arsenic, and sulfur in arsenian pyrite, marcasite, and arsenopyrite to suggest that gold was incorporated into arsenic-rich, iron-deficient surface sites. It is known that pyrite is an effective scavenger for gold in OH-Cl dissolved complex ions relative to goethite (Jean and Bancroft 1985; Schoonen et al. 1992; Scaini et al. 1998). Adsorption onto the surface of pyrite is apparently facilitated by arsenic, which causes pyrite, normally an n-type semiconductor, to become locally a p-type semiconductor (Mironov et al. 1981). The p-type conductivity may be induced by incorporation of chemical impurities, such as arsenic, or by lattice defects (Krendelev et al. 1978; Knipe et al. 1991, 1992). The p-type pyrite would have a stronger electrochemical interaction with negatively charged complex anions (Prokhorov and Lu 1971) such as $Au^{I+}(HS)_2^-$. It has also been suggested that coatings of arsenian pyrite on pyrite could act like p-n junctions, which would have a strong electrostatic character and adsorption potential for gold due to different types of conductivity (Mironov et al. 1981; Möller and Kersten 1994; Möller et al. 1997).

Adsorption of Au^{I+} onto arsenian pyrite probably involves the dominant aqueous gold complexes, $Au(HS)_2^-$ and $Au(HS)^0$. These complexes could combine with S^{2-} that acted as a donor ligand on the surface of arsenian pyrite, forming a tri-atomic surface complex such as S_{py}-Au^{I+}-$S_{bs}H$, in which S_{py} stands for sulfur from the donor ligand on the arsenian pyrite surface and S_{bs} stands for sulfur from the gold-bisulfide complex in the hydrothermal solution. A similar adsorption mechanism has been suggested for deposition of gold on the surfaces of As_2S_3 and Sb_2S_3 (Renders and Seward 1989; Cardile et al. 1993; Tossell 1996). Sha (1993) proposed a related mechanism for deposition of gold on surfaces of arsenian pyrite, and Scaini et al. (1998) reported adsorption of Au^{I+} onto pyrite surfaces from solutions containing Au-HS complexes. Jean and Bancroft (1985), Hyland and Bancroft (1989), Starling et al. (1989), Eggleston and Hochella (1991), Becker et al. (1997), and Scaini et al. (1998) have concluded that chemical reduction of ionic gold to Au^0 usually follows adsorption of aqueous gold complexes on the surfaces of most sulfide minerals. Many of these studies focused on the interaction between sulfide surfaces and fluids in which gold is transported as a chloride complex (Mycroft et al. 1995; Becker et al. 1997). Although this complex is realistic for high temperature systems, where chloride complexes are important in the transport of gold (Sverjensky et al. 1997), it is less likely for most lower temperature hydrothermal systems in which gold is transported as a bisulfide complex. Scaini et al. (1998) also reported the presence of very small aggregates of native gold on the surface of pyrite that has reacted with Au-HS solutions, but note that the higher stability of bisulfide-complexed gold should result in a larger fraction of Au^{I+}.

The amount of Au^{I+} that could enter arsenian pyrite is probably a function of the amount of arsenic present, as well as the crystallographic position and distribution of arsenic in the pyrite structure. If indeed arsenic in arsenian pyrite is confined to the marcasite-like layers mentioned above, then it is likely that Au^{I+} might also be confined to these marcasite-like layers in arsenian pyrite or their contacts with pyrite. Possible reactions for deposition of Au^{I+} in arsenian pyrite and their implications for the genesis of Carlin-type micrometer gold deposits are discussed by Simon et al. (1999).

ACKNOWLEDGMENTS

Support for this study was received from Santa Fe Pacific Gold Corporation (now Newmont Gold Company) and National Science Foundation grant EAR 95-23771 to S.E.K. Additional support was received by G.S. from the International Institute at the University of Michigan and the Institute of International

Education through a Fellowship and a Fulbright grant, respectively. The XANES and EXAFS analyses were carried out at Stanford Synchrotron Radiation Laboratory, which is supported by the Department of Energy, Office of Basic Energy Sciences and the National Institute of Health, Biomedical Research Technology program, and National Center for Research Resources. We thank R.A. Scott for providing unpublished XANES arsenic spectra of Na_3AsO_3. E.J. Essene, J.H. Fortuna, J.R. O'Neil, D.R. Peacor, and L.P. Stixrude provided insightful discussions and critical reviews of various versions of this manuscript.

REFERENCES CITED

Ahrland, S., Nilsson K., Persson, I., Yuchi, A., and Penner-Hahn, J.E. (1989) Formation of gold (I) halide and thiocyanate complexes in pyridine and acetonitrile and the structures of gold (I) solvates in these solvents. A thermodynamic and EXAFS spectroscopic study. Inorganic Chemistry, 28, 1833–1838.

Arehart, G.B., Chryssoulis, S.L., and Kesler, S.E. (1993) Gold and arsenic in iron sulfides from sediment-hosted disseminated gold deposits. Implications for depositional processes. Economic Geology, 88, 171–185.

Bakken, B.M., Hochella, M.F. Jr., Marshall, A.F., and Turner, A.M. (1989) High-resolution microscopy of gold in unoxidized ore from the Carlin mine, Nevada. Economic Geology, 84, 171–179.

Bakken, B.M., Brigham, R.H., and Fleming, R.H. (1991a) The distribution of gold in unoxidized ore from Carlin-type deposits revealed by secondary ion mass spectrometry (SIMS) [abs]. Geological Society of America Abstracts with Programs, 23, 228.

Bakken, B.M., Fleming, R.H., and Hochella, M.F. Jr. (1991b) High-resolution microscopy of auriferous pyrite from the Post deposit, Carlin district, Nevada. In Hausen, D.M. Petruk, W, Hagni, R.D. and Vassiliou, A., eds., Process Mineralogy XI—Characterization of metallugical products. The Minerals, Metals and Materials Society, p. 13–23.

Becker, U., Hochella, M.F. Jr., and Vaughan, D.J. (1997) The adsorption of gold to galena surfaces. calculation of adsorption/reduction energies, reaction mechanisms, XPS spectra, and STM images. Geochimica Cosmochimica Acta, 61, 3565–3586.

Cardile, C.M., Cashion, J.D., McGrath, A.C., Renders, P., and Seward, T.M. (1993) ^{197}Au Mössbauer study of Au_2S and gold adsorbed onto As_2S_3 and Sb_2S_3 substrates. Geochimica Cosmochimica Acta, 57, 2481–2486.

Cathelineau, M., Boiron, M., Hollinger, P., Marion, P., and Denis, M. (1989) Gold in arsenopyrites. crystal chemistry, location and state, physical and chemical conditions of deposition. Economic Geology Monograph 6, 328–341.

Chao, E.C.T., Minkin, J.A., Back, J.M., Chen, J.R., Bagby, W.C., Rivers, L.M., Sutton, S.R., Hanson, A.L., Gordon, B.M., and Jones, D.W. (1986) Occurrence of gold in an unoxidized Carlin-type ore sample—a preliminary synchrotron and micro-optical restudy. Geological Society of America Abstracts with Program, 18, 562.

Chryssoulis, S.L. (1990) Detection and quantification of "invisible" gold by microprobe techniques. In D.M. Hausen, Ed., Gold '90, Society of Mining Engineers, 323–332.

Clark, L.A. (1960) The Fe-As-S system; phase relations and applications. Economic Geology, 55, 1345–1381 and 1631–1652.

Cline, J.S., Hofstra, A., Landis, G., and Rye, R.O. (1997) Ore fluids at the Getchell, Carlin-type gold deposit, north-central Nevada. Society of Economic Geologists Field Trip Guidebook, 28, 155–166.

Cook, N.J. and Chryssoulis, S.L. (1990) Concentrations of "invisible" gold in the common sulfides. Canadian Mineralogist, 28, 1–16.

Couderec, J.-J., Bras, J., Fagot, M., and Levade, C. (1980) Etude par microscopie electronique en transmission de l'etat de deformation de pyrites de differentes provenances. Bulletin Mineralogie, 103, 547–557.

Eggleston, C.M. and Hochella, M.F. Jr. (1991) Scanning tunneling microscopy of galena (100) surface oxidation and sorption of aqueous gold. Science, 254, 983–986.

Elder, R.C. and Eidsness, M.K. (1987) Synchrotron X-ray studies of metal-based drugs and metabolites. Chemical Reviews, 87, 1027–1046.

Fayard, M., Gratias, D., and Portier, R. (1980) Modele de default d'empilement dans la pyrite. Philosophical Magazine, A41, 125–128.

Fleet, M.E. and Mumin, A.H. (1997) Gold-bearing arsenian pyrite and marcasite and arsenopyrite from Carlin trend gold deposits and laboratory synthesis. American Mineralogist, 82, 182–193.

Fleet, M.E., MacLean, P.J., and Barbier, J. (1989) Oscillatory-zoned As-bearing pyrite from strata-bound and stratiform gold deposits, an indicator of ore fluid evolution. In R.R. Keays, W.R.H. Ramsay, and D.I. Groves, Eds., The Geology of Gold Deposits: The perspective in 1988. Economic Geology Monograph 6, 356–362.

Fleet, M.E., Chryssoulis, S.L., MacLean, P. J., Davidson, R., and Weisener, C.G. (1993) Arsenian pyrite from gold deposits. Au and As distribution investigated by SIMS and EMP, and color staining and surface oxidation by XPS and LIMS. Canadian Mineralogist, 31, 1–17.

Friedl, J. (1993) Untersuchungen an Goldmineralen und goldhaltigen Erzen mittels Mössbauerspektroskopie. Thesis, Technical University of Munich, Munich, Germany, 149.

Friedl, J., Paniagua, A., and Wagner, F.E. (1991) Mössbauer study of gold-bearing villamaninite. Neues Jahrbuch für Mineralogie, Abhandlungen, 163, 247–354.

Friedl, J., Wagner, F.E., and Wang, N. (1995) On the chemical state of combined gold in sulfidic ores—conclusions from Mössbauer source experiments. Neues Jahrbuch für Mineralogie, Abhandlungen, 169, 279–290.

Hausen, D.M. (1981) Process mineralogy of auriferous pyritic ore at Carlin, Nevada. In D.M. Hausen, and W.C. Park, Eds., Process mineralogy, extractive metallurgy, mineral exploration, energy resources, p. 271–289. Metallurgical Society of AIME, Warrendale, Pennsylvania.

Hausen, D.M. and Kerr, P.F. (1968) Fine gold occurrence at Carlin, Nevada. In J.D. Ridge, Ed., Ore Deposits of the United States, p. 908–940. Metallurgical Society of AIME, Warrendale, Pennsylvania.

Hausen, D.M. and Park, W.C. (1985) Observation on the association of gold mineralization with organic matter in Carlin-type ores. Denver Region Exploration Geological Society Symposium Proceedings, 3, 119–136.

Hausen, D.M., Ahlrichs, J.W., Mueller, W., and Park, W.C. (1987) Particulate gold occurrences in three Carlin carbonaceous ore types. In R.D. Hagni, Ed., Process mineralogy VI, p. 193–214. Metallurgical Society of AIME, Warrendale, Pennsylvania.

Hirsch, H., De Cugnac, A., Gadet, M.C., and Pouradier, J. (1966) Cristallographie de sulfure aureux, Comptes Rendus de L'Academie des Sciences de Paris, 263, 1327–1330. (in French) **{Auth: ok?}**

Hyland, M.M. and Bancroft, G.M. (1989) An XPS study of gold deposition at low temperature on sulfide minerals, reducing agents. Geochimica Cosmochimica Acta, 53, 367–372.

Jean, G.E. and Bancroft, G.M. (1985) An XPS and SEM study of gold deposition at low temperatures on sulfide mineral surfaces, concentration of gold by adsorption/reduction. Geochimica Cosmochimica Acta, 49, 979–987.

Kettler, R.M. (1990) Organic matter in hydrothermal systems. Implications for fluid chemistry and source, p. 214. Unpublished Ph.D. thesis, Ann Arbor, University of Michigan.

Knipe, S.W., Foster, R.P, and Stanley, C.J. (1991) Hydrothermal precipitation of precious metals on sulfide substrates. In E.A. Ladeira, Ed., Brazil Gold '91. The Economics, Geology, Geochemistry, and the Genesis of Gold Deposits, Rotterdam, Balkema, 431–435.

Knipe, S.W., Foster, R.P, and Stanley, C.J. (1992) The role of sulfide surfaces in the sorption of precious metals from hydrothermal fluids. Institution of Mining and Metallurgy Transactions, Section B, Applied Earth Sciences 101, B83–B88.

Krendelev, F.P., Zhmodik, S.M., Mironov, A.G. (1978) A ^{195}Au study of the sorption of gold by natural layer silicates and iron hydroxides. Geochemistry International, 15, 156–162.

Marion, P.H., Regnard, J.-R., and Wagner, F.E. (1986) Étude de l'état chimique de l'or dans des sulfures aurifèrs par spectroscopie Mössbauer de ^{197}Au. Academie de Sciences (Paris) Comptes Rendus, 302 II, 571–574.

Marion, P.H., Hollinger, P., Boiron, M.C., Cathelineau, M., and Wagner, F.E. (1991a) New improvements in the characterization of refractory gold in pyrites. an electron microprobe, Mössbauer spectrometry and ion microprobe study. In E.A. Ladeira, Ed., Brazil Gold '91. Proceedings of the Symposium Brazil Gold '91, Belo Horizonte, Brazil, May 13–17, 1991, Balkema, Rotterdam, 389–395.

Marion, P.H., Monroy, M., Hollinger, P., Boiron, M.C., Cathelineau, M., Wagner, F.E., and Friedl, J. (1991b) Gold bearing pyrites: a combined ion microprobe and Mössbauer spectrometry approach. In M. Pagel and J. Leroy, Eds., Source, Transport and Deposition of Metals, Balkema, Rotterdam, 677–680.

Mironov, A.G., Zhmodik, S.M., and Maksimova, E.A. (1981) An experimental investigation of sorbtion of gold by pyrites with different thermoelectric properties. Geochemistry International, 18, 153–160.

Möller, P. and Kersten, G. (1994) Electrochemical accumulation of visible gold on pyrite and arsenopyrite surfaces. Mineralium Deposita, 29, 404–413.

Möller, P., Sastri, C.S., Kluckner, M., Rhede, D., and Ortner, H.M. (1997) Evidence for electrochemical deposition of gold onto arsenopyrite. European Journal of Mineralogy, 9, 1217–1226.

Mues, C. and Schuster, H.-U. (1980) Na_2AuAs, Na_2AuSb, K_2AuSb-drei neue A_2BX-Berbindungen mit B-X-Kettenstruktur. Zeitschrift für Naturforschung, 35, 1055–1058.

Mycroft, J.R., Bancroft, G.M., McIntyre, N.S., and Lorimer, J.W. (1995) Spontaneous deposition of gold on pyrite from solutions containing Au(III) and Au(I) chlorides. Part I. A surface study. Geochimica Cosmochimica Acta, 59, 3351–3365.

Nesbitt, H.W., Muir, I.J., and Pratt, A.R. (1995) Oxidation of arsenopyrite by air-saturated distilled water, implications for mechanisms of oxidation. Geochimica Cosmochimica Acta, 59, 1773–1783.

Prokhorov, V.G. and Lu, L.V. (1971) Electrochemical and thermoelectric properties of pyrite as a criterion of the conditions of mineral formation. In Mineralogiya i mineralogicheskaya kristallografiya (Mineralogy and Mineral Crystallography), Sverdlovsk, 115.

Radtke, A.S. (1985) Geology of the Carlin gold deposit, Nevada. U.S. Geological Survey Professional Paper 1267, 124.

Radtke, A.S., Taylor, C.M., and Christ, C.L. (1972) Chemical distribution of gold and mercury at the Carlin deposit, Nevada. Geological Society of America Abstracts with Program, 4, 632.

Renders, P.J.,and Seward, T.M. (1989) The adsorption of thio gold(I) complexes by amorphous As_2S_3 and Sb_2S_3 at 25 and 90°C. Geochimica Cosmochimica Acta, 53, 255–267.

Scaini, M.J., Bancroft, G.M., and Knipe, S.W. (1998) Reactions of aqueous Au^{1+} sulfide species with pyrite as a function of pH and temperature. American Mineralogist, 83, 316–322.

Schoonen, M.A.A., Fischer, N.S., and Wente, M. (1992) Gold sorption onto pyrite and goethite; a radiotracer study. Geochimica Cosmochimica Acta, 56, 1801–1814.

Sha, P. (1993) Geochemistry and genesis of sediment-hosted disseminated gold mineralization at the Gold Quarry mine, Nevada. Ph.D. dissertation, University of Alabama, Tuscaloosa, 228.

Simon, G., Kesler, S.E., Peltonen, D.R., Chryssoulis, S.L., Huang, H., and Penner-Hahn, J.E. (1997) Relation between pyrite and gold at the Twin Creeks SHMG deposit, Nevada. Society of Economic Geologists Field Trip Guidebook, 28, 137–139.

Simon, G., Kesler, S.E., Chryssoulis, S.L., Huang, H., and Penner-Hahn, J.E. (1999) Geochemistry and textures of gold-bearing arsenian pyrite, Twin Creeks Carlin-type gold deposit, Nevada. implications for gold deposition. Economic Geology (in press)

Starling, A, Gilligan, J.M., Carter, J.M., Foster, A.H.C., and Saunder, R.A. (1989) High-temperature hydrothermal precipitation of precious metals on the surface of pyrite. Nature, 340, 298–300.

Stenger, D.P., Kesler, S.E., Peltonen, D., and Tapper, C.J. (1998) Deposition of gold in Carlin-type gold deposits. The role of sulfidation and decarbonation at Twin Creeks, Nevada. Economic Geology, 93, 201–216.

Sverjensky, D.A., Shock, E.L., and Helgeson, H.C. (1997) Prediction of the thermodynamic properties of aqueous metal complexes to 1000C and 5kb. Geochimica Cosmochimica Acta, 61, 1359–1412.

Tossell, J.A. (1996) The speciation of gold in aqueous solution: A theoretical study. Geochimica Cosmochimica Acta, 60, 17–29.

Tossell, J.A., Vaughan, D.J., and Burdett, J.K. (1981) Pyrite, marcasite, and arsenopyrite type minerals. crystal chemical and structural principles. Physics and Chemistry of Minerals, 7, 177–184.

Wagner, F.E., Marion, P.H., and Regnard, J.-R. (1986) Mössbauer study of the chemical state of gold in gold ores. Gold 100, Proceedings of the International Conference on Gold, 2. Extractive Metallurgy of Gold; SAIMM, Johannesburg, 435–443.

——(1988) ^{197}Au Mössbauer study of gold ores, matters, roaster products and gold minerals. Hyperfine Interactions, 41, 851–854.

Wagner, F.E., Marion, P.H., and Swash, P.M. (1989) Mössbauer spectroscopy in the study of chemical state of gold in gold ores. In A. Fuganti, and G. Morteani, Eds., Workshop on Rare and Precious Metals, Castel Ivano, Italy, June 1989. Extended Abstracts, 82–97.

Wells, J.D. and Mullens, T.E. (1973) Gold-bearing arsenian pyrite determined by microprobe analyses, Cortez and Carlin gold mines, Nevada. Economic Geology, 68, 187–201.

MANUSCRIPT RECEIVED SEPTEMBER 14, 1998
MANUSCRIPT ACCEPTED FEBRUARY 13, 1999
PAPER HANDLED BY KATHRYN L. NAGY